Digital Object Identifier 10.1109/ACCESS.2021.3119581

Equivalent Electric and Heat-pump Water Heater Models for Aggregated Community-level Demand Response Virtual Power Plant Controls

HUANGJIE GONG, (Student Member, IEEE), TIM ROONEY*, OLUWASEUN M. AKEYO, (Member, IEEE), BRIAN BRANECKY*, and DAN M. IONEL, (Fellow, IEEE)

ECE Department, University of Kentucky, Lexington, KY, USA
* A. O. Smith Corporation, Milwaukee, WI, USA

Corresponding author: Dan M. Ionel (e-mail: dan.ionel@ieee.org).

ABSTRACT Advanced control techniques may be used to establish a virtual power plant to regulate the operation of electric water heaters, which may be regarded as a "uni-directional battery" and a major component of a hybrid residential energy storage system. In order to estimate the potential of regulating water heaters at the aggregated level, factors including user behavior, number of water heaters, and types of water heaters must be considered. This study develops generic water heater load curves based on the data retrieved from large experimental projects for resistive electric water heaters (EWHs) and heat pump water heaters (HPWHs). A community-level digital twin with scalability has been developed to capture the aggregated hot water flow and average hot temperature in the tank. The results in this paper also include the "energy take" in line with the CTA-2045 standard and Energy Star specification. The data from the experiments demonstrated that changing from an EWH to an HPWH reduces electricity usage by approximately 70%. The case study showed that daily electricity usage could be shifted by approximately 14% and 17% by EWH and HPWHs, respectively, compared to their corresponding average power. Another case study showed that both EHWs and HPWHs, coordinated with PV to reduce morning and evening peaks, could shift approximately 22% of the daily electricity.

INDEX TERMS Electric Water Heater (EWH), Heat Pump Water Heater (HPWH), Digital Twin, Generic Curve, Load Profile, Aggregated Community Load, CTA-2045, Energy Storage, Energy Take, Demand Response (DR), Distributed Energy Resources (DER), Virtual Power Plant (VPP), Smart Home, Smart Grid.

I. INTRODUCTION

THE ubiquity of electric water heaters (EWHs) make them one of the most advantageous appliances for participation in the virtual power plant (VPP) operation for residential buildings. The EWHs have large thermal masses of water in their tanks and can be regarded as both heat reservoirs and energy sinks. Their effective tank insulation gives high equivalent thermal resistance compared to pipes, resulting in less energy loss associated with water heater tanks than distribution systems [1].

These properties allow EWHs to, for a short period of time, be turned OFF for load shedding while maintaining the water temperature at the reference temperature. Furthermore, EWHs can be used to absorb surplus PV generation. As PV penetration keeps rising, there are multiple benefits of incorporating EWHs into home energy management. Recent research indicates that battery capacity may be reduced by up to 30% when batteries are coordinated with EHW, which were regarded as "uni-directional" energy storage [2].

The electric water heater accounts for a substantial portion of a typical house electric power consumption [3]. However, the unpredictability of customer behavior makes quantifying the benefits of controlling EWHs difficult. Demand response (DR) implementations must carefully balance the water temperature in the tank to provide the maximum grid benefit between two bounds, i.e., it must be kept high enough to meet the user demand while not exceeding the stipulated safety reference. Fortunately, technologies such as mixing valves

may be used to allow the water to be safely stored up to 145F and still meet safety requirements [4], [5].

The power profile of water heaters is largely decided by user behavior. In previous studies, the hot water draws for 48 representative days were evaluated based on measured data from California homes [6]. The proposed schedules are used in the California Building Energy Code Compliance for Residential buildings (CBECC-Res) [7]. In another study, the aggregated EWH load was calculated by analyzing the hot water usage schedules [8]. A typical aggregated load for EWHs has a morning and evening peak, as shown in the study involving 50 water heaters [9]. The aggregated load curve for the resistive EWHs was proposed in a previous conference paper by the same group of authors [10].

Residential water heaters have large thermal masses and can provide ancillary services with relatively low-cost [11], [12]. These services could improve the reliability of the grid and provide monetary benefits to both the grid and residences while maintaining user comfort [13]–[17]. The potential regulation capacity of water heaters is impacted by factors including ambient temperature, hot water usage, and setpoint [18]–[21].

An internet-based survey involving 1,600 members found that approximately 70% of the residential participants would allow the utility to control their switches or thermostats when proper incentives were provided [22]. The potential of water heater related technologies was widely appreciated in the annual conference of Hot Water Forum held by the American Council for an Energy-Efficient Economy (ACEEE) [23]. Topics including the EWH modeling, optimization, and related market investigations for the benefit of industry, utilities, and research institutes were addressed in the forum.

A universal port for smart products, including water heaters, was designed by the Consumer Technology Association (CTA) and well known as CTA-2045 standard [24], [25]. The CTA-2045 standard can potentially meet the challenges in the large employment of smart devices, including differences between products across manufacturers and data streaming. In principle, the Energy Star [26] and CTA-2045 standard define a set of functional requirements such as "normal operation", "shed", "load up", etc., and a set of specifications and concepts such as "energy capacity", "energy content", and "energy take". Those specifications and functional requirements can be extended to any energy storage device, enabling a unified approach at the system level. For EWH, success has been reported at the individual residential and utility aggregated levels [12], [27].

Major research gaps remain and a representative power profile for aggregated water heater load that can be scaled to any number is yet to be developed. This is essential to estimating the potential of DR at the power system level. Also, EWHs and HPWHs have very different characteristics so they need to be analyzed separately. While inlet and outlet temperatures are easy to measure, they do not represent stored energy well as the temperature inside the water tank is stratified [27].

Fig. 1: The illustrative parts of A.O.Smith "Energy Smart" model and CTA-2045 standard port. The "Energy Smart" controller is smart grid ready and implements standardized communications for demand response.

The major contributions of this paper include: (1) the development of generic load curves for daily electricity usage of EWH and HPWH based on data retrieved from two large scale projects, respectively; (2) a community level digital twin for water heaters with scalability to any number, which involves the hot water flow, water temperature in the tank, and "energy take"; (3) quantification of the potential of load shifting for both EWH and HPWH under different scenarios.

Following the Introduction: the large-scale experimental studies for EWH and HPWH are presented in Section II and III, respectively. The digital twin water heater model is proposed in Section IV. In Section V, the DR example is carried out for constant power. The DR case for harvesting the energy capacity of the water heater is presented In Section VI. The conclusions are provided in the last section.

II. LARGE SCALE EXPERIMENTAL STUDY FOR ELECTRIC WATER HEATER

A smart EWH that allows users to control the setpoint, the operating mode and receive alerts based on the device operation was developed by A.O. Smith. Approximately 800 anonymized units with the "Energy Smart" EWH controller were analyzed in the program, in which appliance usage data were retrieved and evaluated. The "Energy Smart" controller can be plugged into the EWH and enables the monitoring, remote control, alarming, and creating custom heating schedules [28]. The EWH heater models optionally include a CTA-2045 port adapter and utility communication module to enable smart communication with energy providers (Fig. 1).

Over a two-year period from 2018 to 2020, the data analyzed witnessed a growing number of participants, peaking at nearly 500 electric water heaters recorded per day in early 2019 (Fig. 2). Based on the data retrieved, up to 100 participants opted out of the program at inception and 140 EWHs participated through the entire length of the project (Fig. 3). During the project span, approximately 350 EWHs were reporting their instantaneous power online.

The daily power profile for EWHs is determined by the user-influenced parameters such as hot water usage and the

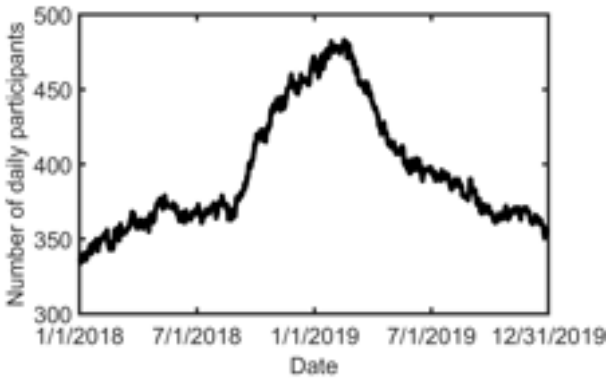

Fig. 2: Daily number of EWH in service. Approximately 800 participants were analyzed as part of the program and an increase from 2018 till early 2019 can be observed before the gradual decline.

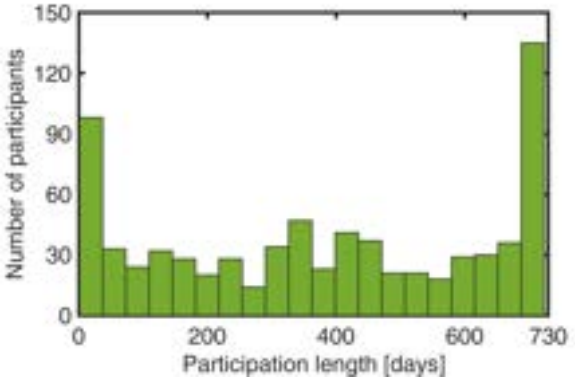

Fig. 3: Participant engagement over the duration of the research. Reduction in the number of participants in some cases were attributed to changes in internet settings and monitoring hardware devices being disconnected.

hot water temperature set point. The power profile for EWHs is also influenced by other factors including the ambient temperature, inlet water temperature, and the insulation of domestic water pipes. Hence, there is variation in the power curve from one EWH unit to the other. A typical residential EWH would normally have two or three short heating cycles daily, leading to sharp power differences throughout the day. Only when the number of EWHs being analyzed is fairly large is the aggregated EWH power relatively smooth with distinct trends.

The experimental data was reported in Coordinated Universal Time (UTC) but the location of the EWH was not recorded. This is because all the user information had been anonymized in order to protect privacy. As the data was collected within the entire continental USA, the time zone for the experimental data is regarded as UTC-06:30, i.e., between the CST and MST.

Table 1: The p.u. value of average EWH power

Hour	0	3	6	9	15	18	20
Power [p.u.]	0.33	0.33	1.5	1	0.75	1.25	1.25

At each minute, the aggregated EWH load was calculated by summing all the selected power together. The base power, which is used to calculate the per unit value, is defined as follows:

$$P_{base} = \frac{E \cdot N}{T}, \tag{1}$$

where, E is the average daily electricity usage; N, the total number of EWHs; and T, representing the number of hours to be averaged over. In this paper, E is fixed to 12.5kWh as the typical daily electricity usage for EWH and T is fixed to 24, for the number of hours in one day. In the case of HPWHs, E is also 12.5kWh so the per-unit load values for both EWH and HPWH are comparable. The actual energy produced by EWHs and HPWHs is assumed to be the same. For the HPWH, the Coefficient Of Performance (COP) is defined as the ratio between the power drawn out of the HPWH and the power supplied to the compressor. Due to the COP of HPWH, the electricity usage of EWH and HPWH are different.

The per unit value for the aggregated water heater load power is calculated as:

$$P_{pu}(t) = \frac{P_A(t)}{P_{base}}, \tag{2}$$

where P_A is the aggregated water heater power acquired from the measurements at time t.

The measured power profiles were used to develop an aggregated generic load profile to represent the typical power flow for multiple EWHs. The generic EWH load profile was defined by 8 data points for which the mathematical derivative of the load curve, i.e. ramping rate, changes drastically. The data point for hour 24 is not shown because hour 0 and hour 24 have the same value (Table 1). The values between those points were interpolated linearly with user defined resolution. The time step of 1-minute was used throughout this paper if not mentioned otherwise. The generic curve captured the major characteristics of the experimental data, as the peaks, ramping rates, and the power values for different time periods were almost the same (Fig. 4). The aggregated EWH load curves shown in Fig. 4 include the per unit value and an example for 1,000 EWHs for which the base power has been calculated with (1) to be equal to 521kW.

Another experimental study, of a smaller scale with only 50 EWH, has been conducted by the researchers from the Oak Ridge National Laboratory (ORNL) [9]. The results shown in Fig. 5 confirm the typical timing of the morning and evening peaks, which shows the similar trend compared with the generic curve. When comparing data and considering scaling between Figs. 4 and 5, it should be kept in mind that the smaller scale study illustrates the variability due to the day of the week, which can be substantial, and also includes larger power variations possibly due to community/location specifics and the low number of EWH considered. Obtaining substantially large local data for the utility might be a challenge and the corresponding aggregated load based on the limited data might have large variation. On the other hand, the

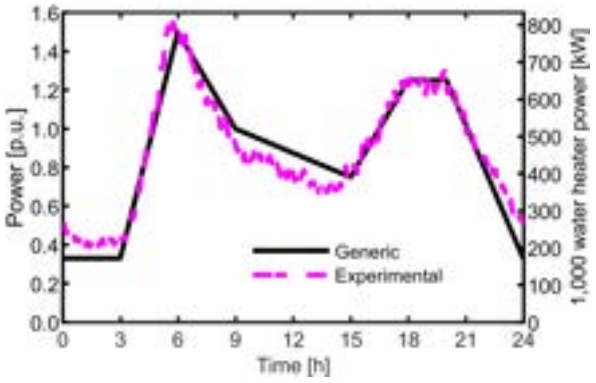

Fig. 4: Example daily aggregated power transfer for EWH. The aggregated generic profile was developed based on data retrieved from the two-year long project.

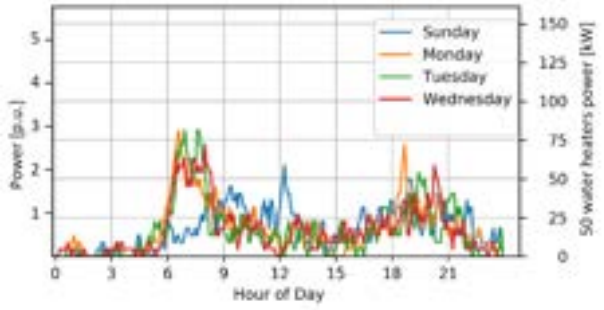

Fig. 5: Experimental aggregated data based on a smaller scale study that included only 50 water heaters [9]. The morning and the evening peaks are approximately timed in line with expectations, as compared with the example generic curve of Fig. 4, and the power values illustrate the community dependent variability.

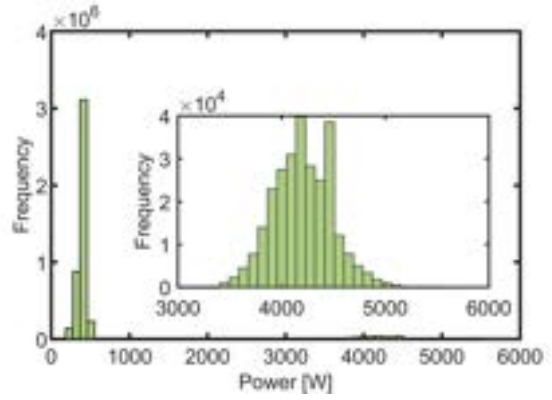

Fig. 6: The distribution for the instances of selected power values. Two clusters stand for the compressor power only and the instances which include the resistance element, which are approximately 94% and 6%, respectively.

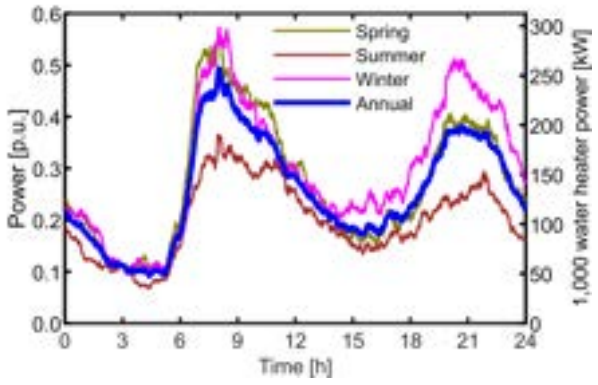

Fig. 7: The generic power curve created based on the BPA data for Spring, Summer, and Winter for the year of 2018. The annual curve, which includes the data from the three seasons, is used to generate the generic HPWH curve.

generic curved proposed in Fig. 4 is artificially aggregated in time and space throughout the entire continental US, which spans four time zones, i.e., UTC-05:00 to UTC-08:00. Therefore, the aggregated load was able to represent the national trend, but needed adjustment when employed to a specific location. The learnings from the two studies can be combined with other locally based statistics to establish a specific load curve for electric power utility DR planning.

III. LARGE SCALE EXPERIMENTAL STUDY OF HEAT PUMP WATER HEATER

The Bonneville Power Administration (BPA) has spent the recent years developing the capability to use the CTA-2045 enabled water heaters for both traditional demand response and everyday applications such as renewable generation integration. The project, which delivered the experimental data used by this paper, deployed 300 CTA-2045 enabled HPWHs in the Pacific Northwest (PNW) over one year. The data has a resolution of 1-minute and covers January through August of 2018 [29].

The data includes multiple columns, among which the `timestap`, `alias`, `curr_curtail_type`, `curr_watts` were used to generate the generic load curve for the HPWH. The `alias` records the device name and distinguishes the type of water heater. This was used in this paper to select only the data from HPWHs. The `curr_curtail_type` records the demand control signal. In this paper, only the days having a signal of `End Shed/Run Normal = 8` for the entire day were selected. Therefore, for the selected days, all their 1,440 records of column `curr_curtail_type` must be 8. The `timestamp` and `curr_watts` record the timestamp and the instantaneous watt reported by the water heaters. Additionally, only the business days were selected as user behavior differs on holidays and weekends.

Approximately 10,000 daily HPWH schedules were selected and each schedule had 1,440 recorded power instances. The distribution for the values of the selected instantaneous power shown in Fig. 6 does not include times without a power draw. When the HPWHs were ON in `End Shed/Run Normal` mode all day long, the compressors were operating alone 94% of the time and, for the other 6% of the time, the resistance element was ON.

The data was provided for three seasons separately, i.e., Winter: Jan-Apr, Spring: Apr-June, and Summer: June-Aug.

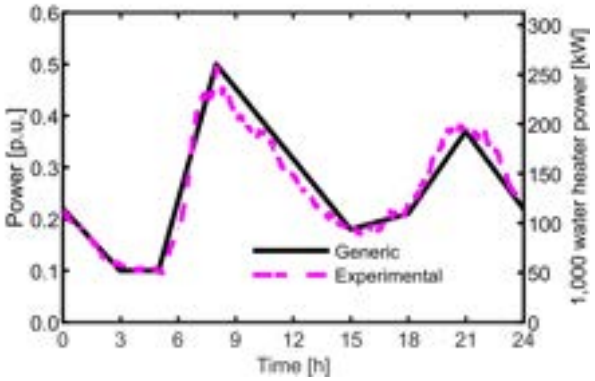

Fig. 8: The experimental and generic curve of the daily HPWH power profile. The experimental curve is based on the same data as the annual curve shown in Fig. 7.

Table 2: The p.u. value of average HPWH power

Hour	0	3	5	8	15	18	21
Power [p.u.]	0.24	0.1	0.1	0.5	0.18	0.21	0.37

The annual curve was calculated by using the data from all three seasons together. It is observed that, even though the peak values differ, all the daily load curves have two peaks at approximately 8am and 9pm, as shown in Fig. 7.

The generic HPWH load curve was created based on the annual load curve presented in Fig. 7 and was defined by 8 data points as in the Table 2. The data for hour 24 is not shown because, as at the end of the day, the value is the same as the beginning. The generic curve based on the annual data is shown in Fig. 8 in both per unit value and the value for 1,000 HPWH.

The experimental data and generic curves for both EWHs and HPWHs are presented together in Fig. 9. The peak value for EWHs is approximately 3 times the peak value for HPWHs. It is observed that the peak for HPWH comes later for both morning and evening. Unless otherwise mentioned, the studies in the rest of this paper are all based on the generic curves.

The per unit value for energy usage is deduced by integrating both side of (2) with respect to time:

$$\int P_{pu}(t)\mathrm{d}t = \int \frac{P_A(t)}{P_{base}}\mathrm{d}t \Rightarrow E_{pu}(t) = \frac{E_A(t)}{P_{base}}, \qquad (3)$$

where $E_A(t)$ is the measured aggregated energy usage. In a per unit system, the base and the actual value have the same unit. Based on (3), the base value for the aggregated energy (MWh) has the same magnitude as P_{base} ($|E_{base}| = |P_{base}|$). The cumulative electricity usage based on the generic load curves for EWH and HPWH are shown in Fig. 10. At the end of the day, the aggregated electricity usage for EWH and HPWH are 21.4 p.u. and 6.3 p.u., respectively. Given 1,000 water heaters, the daily electricity usage for an all EWH community and an all HPWH community are 11,146kWh and 3,281kWh, respectively. For a community changing from all EWH to all HPWH, the daily saving on electricity is approximately 70%.

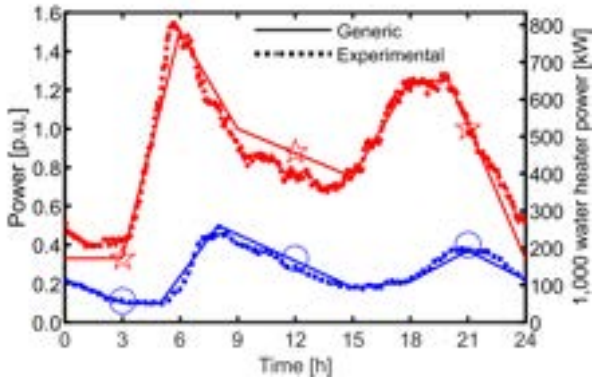

Fig. 9: The experimental and generic curves for both EWHs (indicated with ☆) and HPWHs (indicated with ○) in the same scale.

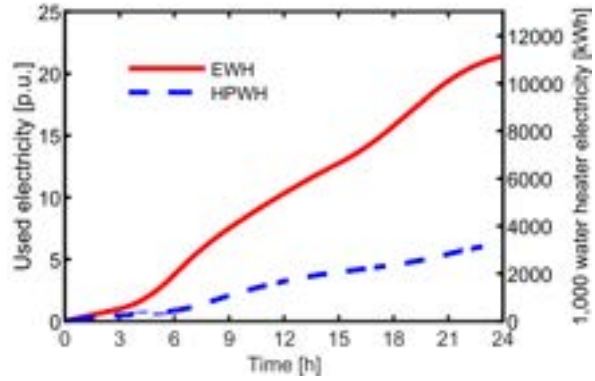

Fig. 10: The accumulated electricity usage for the EWH and HPWH based on the generic load curves. The daily electricity usage for EWH and HPWH are 21.4 p.u. and 6.3 p.u., respectively.

IV. EQUIVALENT EWH AND POSSIBLE MODEL FOR DIGITAL TWIN

One simplification and two assumptions have been made in this paper to facilitate the study. The water temperature in the tank was simplified to be uniform instead of stratified. Simulation results (Fig. 11) based on the simplification are satisfactory when compared with the experimental data. Other models, including the "WaterHeater:Mixed" in EnergPlus [30] and the model used for International Energy Conservation Code (IECC) by the Department of Energy (DOE) and Pacific Northwest National Laboratory (PNNL) [31] all consider uniform temperature tanks appropriate. The models developed by Ecotope [32] consider vertical stratification of the water tanks and have accurate results at the cost of performance. In this paper, the uniform temperature in the water tank was considered as it is sufficient for the evaluation of the energy balance in the water tank.

The first assumption is that COP of the HPWH was constant for the calculation of the daily profile. COP will not change drastically when the ambient environment remains

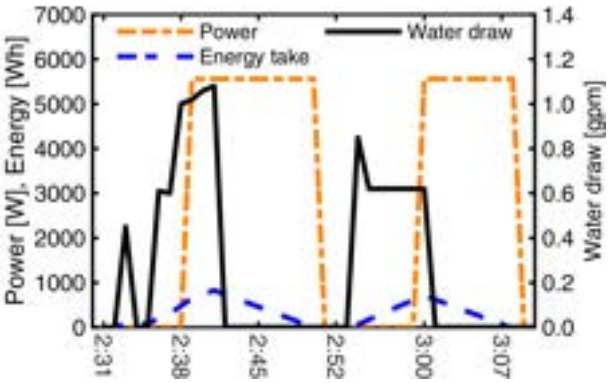

Fig. 11: Simulation results obtained based on (4). The data compares satisfactorily with the experimental results from the NREL test published in the EPRI report [27].

stable, which is the common case for most of residential users. The second assumption is that the average water temperature for all the EWHs whose power was used to generate the generic curve (Fig. 4) was constant when there was no DR control. This assumption was based on basic aggregation, that for a given point in time, some water heaters have high temperature while others have low. Based on these assumptions, the hot water usage and the temperature in the tank for the water heaters can be calculated.

An equivalent thermal model is used to calculate the daily hot water usage based on the generic load. Typically, the water temperature in the tank is stratified. In this paper, the average water temperature is considered sufficient for the estimation of the energy storage capacity of the water heater. Therefore, the thermodynamic of the water heater is represented in a single-nodal model:

$$C\frac{\mathrm{d}\theta_T(t)}{\mathrm{d}t} = S(t)P_H(t) - \frac{1}{R}\left[\theta_T(t)-\theta_A\right] - \rho c_p W(t)\left[\theta_T(t)-\theta_{W,C}\right]. \quad (4)$$

The three terms on the RHS consider the effect of the input electric power, the standby heat loss, and the hot water draw activities, respectively. C and $S(t)$ are the equivalent thermal capacitance and ON/OFF status, defined respectively, as:

$$C = V\cdot\rho\cdot c_p. \quad (5)$$

$$S(t) = \begin{cases} 0, & \text{if } S(t-1)=1 \;\&\; \theta_T(t)\geq\theta_H(t) \\ 1, & \text{if } S(t-1)=0 \;\&\; \theta_T(t)\leq\theta_L(t) \\ S(t-1), & \text{otherwise,} \end{cases} \quad (6)$$

where θ_L and θ_H are the lower and upper band of the water tank temperature. The definitions of other parameters are listed in Table 3. It is worth noting that the water heater heating rate P_H, the water temperature in the tank θ_T and the hot water draw W have only their units listed in the table. Also important is that the water heater heating rate P_H for the HPWH should consider its COP.

Table 3: Parameters for the equivalent EWH model.

Parameter	Value or unit
Density of water ρ	993 $^{kg}/_{m^3}$
Specific heat capacity of water c_p	4,179 $^{J}/_{kg^\circ C}$
Room air temperature θ_A	22 °C
Temperature of cold water $\theta_{W,C}$	10 °C
Water heater heating rate P_H	kW
Water tank volume V	50 gallon
Equiv. thermal resistance R	^{a}1400 $^{\circ C}/_{kW}$ ^{b}600 $^{\circ C}/_{kW}$
Water temperature in the tank θ_T	°C
Hot water flow W	m^3/s

$^a EWH, ^b HPWH$

The performance test of a CTA-2045 equipped A. O. Smith water heater was conducted by National Renewable Energy Laboratory (NREL) and reported by the Electric Power Research Institute (EPRI) [27]. The case of "normal operation" from the report was used for the validation of the parameter values listed in Table 3, where the water heater heating rate, P_H, was set to 5.5kW only for this validation. The simulation results, which were plotted in the same style as the report, show satisfactory results (Fig. 11). The term "energy take" reflects the temperature of the water tank.

The proposed single-nodal model is scalable with its parameters represented in the per unit system. Dividing both sides of (4) by $P_{base}|_{N=1}$ yields:

$$\frac{C}{P_{base}|_{N=1}}\frac{\mathrm{d}\theta_T(t)}{\mathrm{d}t} = S(t)\frac{P_H(t)}{P_{base}|_{N=1}} - \frac{1}{RP_{base}|_{N=1}}\left[\theta_T(t)-\theta_A\right] - \rho c_p\frac{W(t)}{P_{base}|_{N=1}}\left[\theta_T(t)-\theta_{W,C}\right]. \quad (7)$$

When there is only one water heater, the aggregated power is the power of the single water heater:

$$P_A(t) = P_H(t), \quad (8)$$

and the per unit value for the aggregated water heater power in (2) becomes:

$$P_{pu} = \frac{P_H(t)}{P_{base}|_{N=1}}, \quad (9)$$

as $P_{base}|_{N=1} = \frac{E}{T}$, (7) is rewritten as:

$$\frac{CT}{E}\frac{\mathrm{d}\theta_T(t)}{\mathrm{d}t} = S(t)P_{pu}(t) - \frac{1}{RE/T}\left[\theta_T(t)-\theta_A\right] - \rho c_p\frac{W(t)T}{E}\left[\theta_T(t)-\theta_{W,C}\right]. \quad (10)$$

Defining the per unit values as: $C_{pu} = \left|\frac{C\cdot T}{E}\right|, R_{pu} = \left|\frac{R\cdot E}{T}\right|, W_{pu} = \left|\frac{W\cdot T}{E}\right|$, the heat transfer function of a water

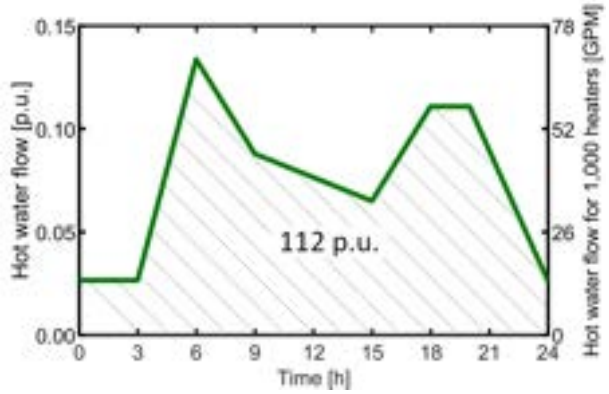

Fig. 12: The calculated aggregated daily hot water flow. The total daily hot water usage was 112 p.u. Given 1,000 water heaters, total daily hot water usage was 58,507 gallons.

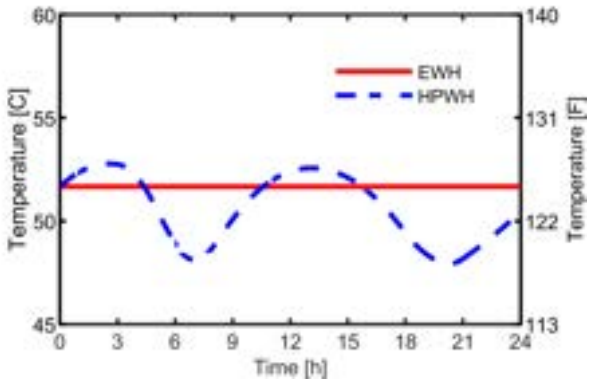

Fig. 13: The average temperature for EWH and HPWH, which were calculated using the same hot water flow and the corresponding generic loads. The constant average temperature value for EWH indicates the instant reaction of the resistance element. The variation in average temperature for HPWH shows the deferring nature of the compressor.

heater is represented as:

$$C_{pu}\frac{\mathrm{d}\theta_T(t)}{\mathrm{d}t} = S(t)P_{pu}(t) - \frac{1}{R_{pu}}[\theta_T(t)-\theta_A] - \rho c_p W_{pu}(t)\left[\theta_T(t)-\theta_{W,C}\right]. \quad (11)$$

The heat transfer function (4) holds for single water heater, therefore, it holds for the average values of $C, P_H(t), R$, and $W(t)$:

$$\overline{C}\frac{\mathrm{d}\theta_T(t)}{\mathrm{d}t} = S(t)\overline{P_H}(t) - \frac{1}{\overline{R}}[\theta_T(t)-\theta_A] - \rho c_p \overline{W}(t)\left[\theta_T(t)-\theta_{W,C}\right]. \quad (12)$$

Rewriting (12) as:

$$C_{pu}\frac{C_{base}}{N}\frac{\mathrm{d}\theta_T(t)}{\mathrm{d}t} = S(t)P_{pu}(t)\frac{P_{base}}{N} - \frac{1}{R_{pu}\frac{R_{base}}{N}}[\theta_T(t)-\theta_A] - \rho c_p W_{pu}(t)\frac{W_{base}}{N}\left[\theta_T(t)-\theta_{W,C}\right]. \quad (13)$$

Compared with (11), the equation (13) holds when $\left|\frac{C_{base}}{N}\right| = \left|\frac{P_{base}}{N}\right| = \left|\frac{1}{R_{base}/N}\right| = \left|\frac{W_{base}}{N}\right|$. Therefore, the base values are defined as: $|C_{base}| = |W_{base}| = |P_{base}|, |R_{base}| = \left|N^2/P_{base}\right|$.

In the study, it is assumed that the average temperature of all the EWHs was constant at $\theta_T(t) = 125F$ due to their fast recovery rate relative to HPWHs. Therefore, (11) can be re-written to calculate the per unit hot water usage:

$$W_{pu}(t) = \frac{S(t)P_{pu}(t) - \frac{1}{R_{pu}}[\theta_T(t)-\theta_A]}{\rho c_p\left[\theta_T(t)-\theta_{W,C}\right]}. \quad (14)$$

The generic load for EWHs is used to calculate the aggregated hot water draw, i.e., the item "$S(t)P_{pu}(t)$" is replaced by the value of the generic load of the EWH at each time point. The calculated generic hot water flow shown in Fig. 12 stands for the representative user behavior and does not change when the water heater is HPWH or the DR is implemented. In this study, the hot water flow has the time resolution of 1-minute and is presented in per unit value as well as gallon per minute (GPM). The daily hot water draw is calculated by integrating the hot water flow with respect to minute, and the results, i.e., the area between x-axis and the curve in Fig. 12 are 112 p.u., and 58,507 gallons for the 1,000 water heater example.

The generic hot water draw and the generic load curves are used to calculate the average tank temperature using (11). As shown in Fig. 13, the average tank temperature for EWH is constant as expected. The variation in the average temperature for HPWH reflects its latent nature.

The equivalent water heater model may be thought of as a digital twin for three reasons. First, all the I/O can be real-time if the data is available. Second, the model can stream data complying to the communication protocol approved by CTA-2045 standard. Third, the model is exchangeable with the hardware in a co-simulation circumstance where the EWH is involved as one of the smart components. Example applications can be found in the Distributed Energy Resources (DER) integration testbed developed by EPRI [33]. This paper focuses on the computational parts of the EWH model while the data packing and communication will be introduced in future work.

V. CONSTANT POWER OPERATION USING LOAD SHIFTING

In the ideal case, the aggregated water heater loads can be kept constant by shifting the peaks, as illustrated in Fig. 14. The electricity used at peak load period, which is above the average power and marked with "•" can be shifted to the time when the power is low, as the areas marked with "▲". In this study, for the EWH, 3.1 p.u. of energy, which was 14% of daily electricity usage, could be shifted with the reference to the average power. For HPWH, the numbers are 1.1 p.u. and

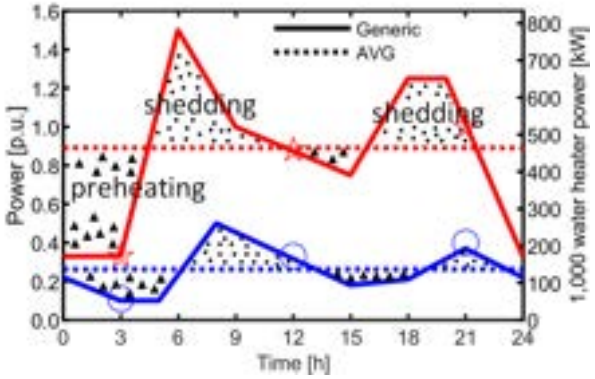

Fig. 14: The illustration for shifting the water heater load to operate on the average power. The COP = 3.4 is calculated based on of the two average powers. With the reference to the average power, the EWH and HPWH could shift approximately 14% and 17% of their corresponding daily electricity usage, respectively.

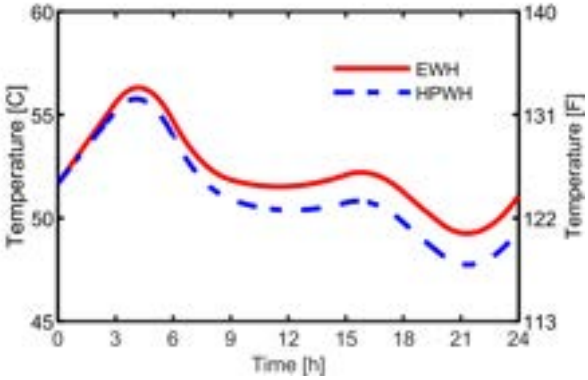

Fig. 16: The average temperature for EWH and HPWH, which were calculated using the same water draw and the corresponding constant power. The input energy for EWH and HPWH were the same all the time. After the starting point, the HPWH always had lower tank temperature because of higher heat loss.

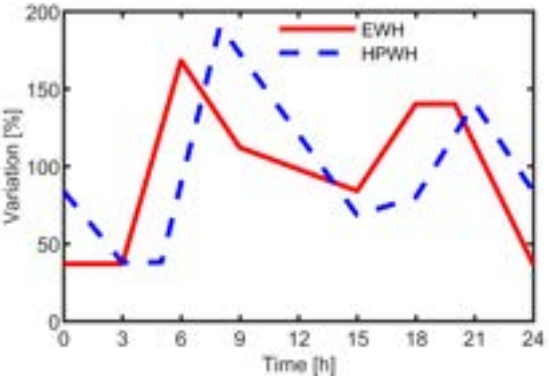

Fig. 15: The relative values of EWH and HPWH generic load power compared with their corresponding average value. The HPWH has larger variation.

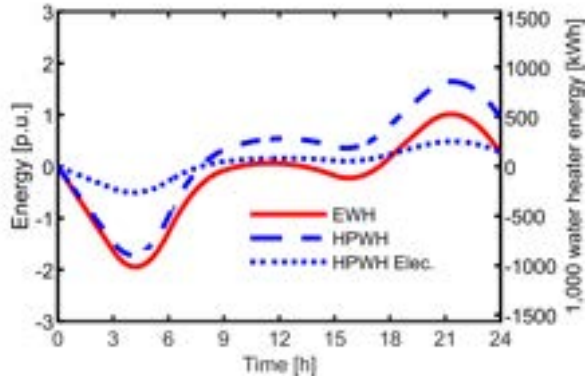

Fig. 17: The energy take for EWHs and HPWHs for the same water draw and the corresponding average power. The energy take for HPWHs was more than that of EWHs when they had the same amount of input energy due to higher heat loss. The HPWHs use less electricity to heat the water because of their COP.

17%.

By preheating and shedding, both EWH and HPWH can work on the constant powers, which are the average powers. It is assumed that both EWH and HPWH have the same amount of input energy for water heating. Therefore, the portion between the two average powers is regarded as the COP for the aggregated HPWH, which is 3.4.

The absolute power of the aggregated HPWHs is lower in general when the numbers of EWHs and HPWHs are the same. However, further inspection reveals that the power profile of HPWHs has a larger variation with the reference to the average power (Fig. 15). In communities where HPWHs are widely installed, shifting the water heater loads can reduce the peak power demand significantly.

The water heater digital twins were used to calculate the average water temperature in the tank and monitor the user comfort. The hot water flow remains unchanged as the user behavior will not change. The preheating and shedding procedures change the hot water temperature in the tank. When the aggregated water heater powers were constant, the average water temperatures in the tank were calculated according to (11) and presented in Fig. 16. For both EWHs and HPWHs, the tank temperatures were above the minimum required 115F when the aggregated heating power was constant. Due to the COP, the input energy for heating the water were the same for both EWH and HPWH at any moment even the HPWH used less electricity. The average tank temperature for HPWH was always lower because of higher standby losses to ambient. It is worth noting that even the HPWHs have higher standby losses to ambient, their overall efficiency is much higher than that of the EHWs due to the COP.

Measuring the temperature in the water tank requires sophisticated techniques as water with different temperature is stratified and is not mixed evenly. Water heaters that are CTA-2045 ready can monitor the devices with the readable quantities related to energy. According to the Energy Star specification, the "energy content of the stored water" for water heater, E_W, is calculated as:

$$E_W(t) = V\rho c_p \theta_T(t), \tag{15}$$

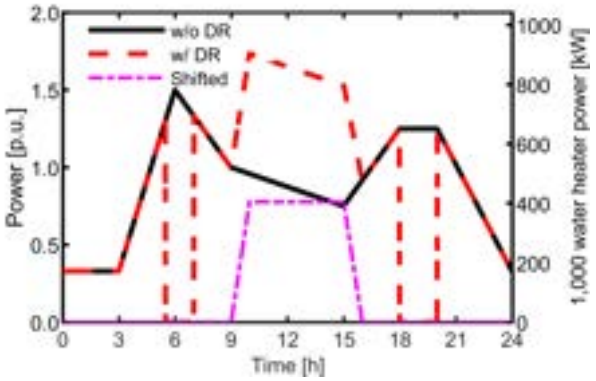

Fig. 18: Example demand response for aggregated EWH based on the generic load. This approach demonstrates how the peak demand of aggregated EWH load at the morning and evening peaks can be shifted to midday, when solar generation is relatively high.

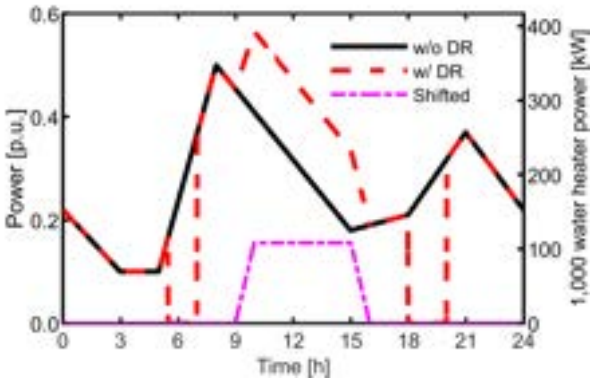

Fig. 19: Example demand response for aggregated HPWH based on the generic load. The shedding periods for the HPWH were selected as the same as that of the EWH case for comparison.

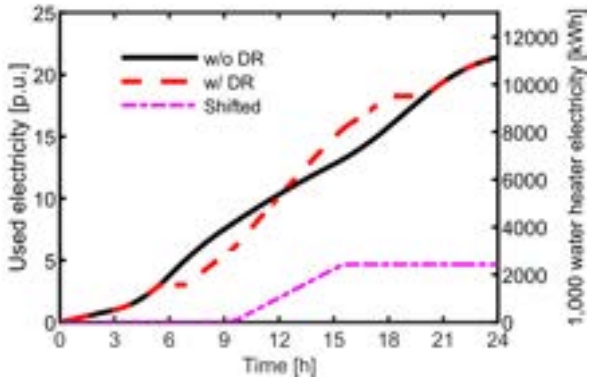

Fig. 20: Accumulated electricity usage of the aggregated EWH. Both cases used the same amount of total electricity at the end of the day, which was 21.4 p.u. In the DR case, the electricity usage remained unchanged during the morning and evening peak shedding period. The electricity usage for the DR case increased fast in the afternoon due to the shifted electricity.

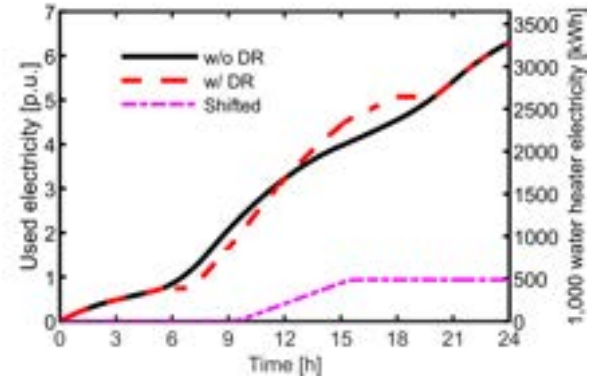

Fig. 21: Accumulated electricity usage of the aggregated HPWH. During the morning and evening peak shedding period, the used electricity remained unchanged in the DR case. More electricity was used in the afternoon due to the load shifting. Both cases used the same amount of electricity at the end of the day, which was 6.3 p.u.

where θ_T is the water temperature, and other parameters are listed in the Table 3. The energy take between two time points is calculated as:

$$ET_W(t_1 - t_2) = E_W(t_1) - E_W(t_2). \tag{16}$$

In this paper, the energy take at one time point was defined as the difference between the "energy content of the stored water" in that time point and that of the zero (0) time point.

The energy take for EWHs and HPWHs under constant power is shown in Fig. 17. The negative values in the early morning indicate the preheating procedure, during which energy was put into the water tank instead of being taken out. The energy take for HPWHs was higher due to higher heat loss. Because of the COP, the corresponding electricity for HPWHs had a much lower value, as presented in Fig. 17.

VI. DEMAND RESPONSE STUDY FOR MORNING AND EVENING

The objective of demand response is to shed the EWH load at critical time, and recover during the midday, as follows:

$$P_D(t) = \begin{cases} P_T, & \text{if } t \in T_D \\ P_O(t) + P_R(t), & \text{if } t \in T_R, \end{cases} \tag{17}$$

where P_D is the aggregated EWH load with DR; P_T, the target aggregated power; P_O, the original aggregated EWH load without DR; P_R, the shifted power; T_D, the set of time when DR is required; T_R, the set of time when the power is shifted to.

CTA-2045 provides energy take as an alternative to temperature control. The most useful value, i.e., the amount of energy that can be stored, is provided to the utility, and details of temperature control can be avoided. Adjusting the temperature bounds of the water heater can maximize the energy storage capability. However, for the concerns regarding safety and user comfort, the residences are not encouraged to

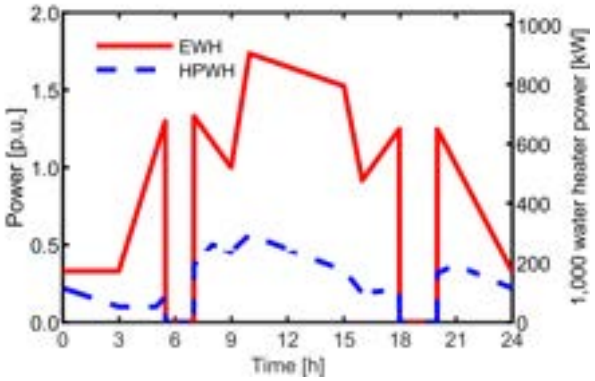

Fig. 22: The aggregated power for EWH and HPWH with DR control. The morning and evening peaks for both EWH and HPWH were shifted to the afternoon when the PV had surplus generation.

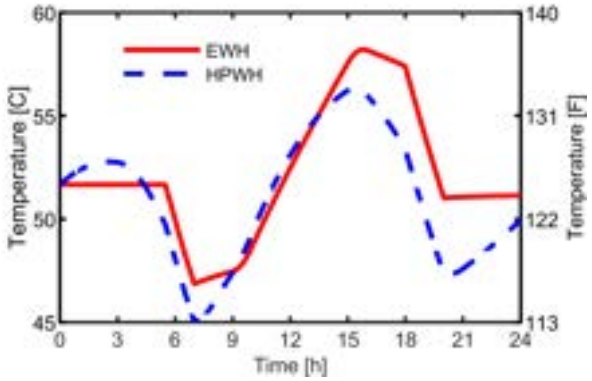

Fig. 23: The average hot water temperature in the tank for both EWH and HPWH with DR control. The example shows a significant reduction in tank temperature in the early hours for the extreme condition when all the water heaters were turned OFF. The recovery around midday means the water heaters can be used as storage for surplus PV generation.

change the set points, which are defined by the manufacturers with specific knowledge of tank geometry and sensor readings [34]. The case studies in this paper represent the utility-controlled DR load type, instead of consumer-incentive DR control. Similar to industrial shedding, an extreme scenario was carried in this paper to evaluate the potential of energy storage capacity of EWHs and HPWHs.

In this study, the generalized characteristics of residential PV was considered and the EWH and HPWH reserved the energy storage capacity for the afternoon. The aggregated power for an example demand response with $T_D = [5:30, 7:00] \bigcup [18:00, 20:00]$, $T_R = [9:00, 16:00]$ and $P_T = 0$ for EWH is shown in Fig. 18. In this extreme example case, the loads at morning and evening peaks were entirely shifted to the afternoon. The same shedding periods were selected for HPWH for comparison and results are shown in Fig. 19.

The electricity usage for both EHW and HPWH are shown in Fig. 20 and 21, respectively. For both EWH and HPWH, during the shedding periods, the electricity usage remained unchanged. In the DR case, the electricity usage increased faster due to the shifted load starting from 9am. For both with and without DR case, the total electricity usage was the same at the end of the day.

The aggregated power profiles for EWH and HPWH under DR control are shown together in Fig. 22. The fixed hot water flow from Fig. 12 was used for the DR study for both EWH and HPWH. During the shedding period in the morning, which stands for the maximum load reduction case scenario, the water temperature in the tank dropped significantly, as shown in Fig. 23. The water temperature for HPWH dropped even below the minimum 115F under the extreme shedding case. A practical home energy management would put the customer comfort as priority and avoid the tank temperature being too low. The high water temperature in the afternoon was feasible due to the implementation of mixing valve technology.

The corresponding energy take is shown in Fig. 24 for the demand response case. For both EWHs and HPWHs, the shedding in the morning led to high energy take, leaving

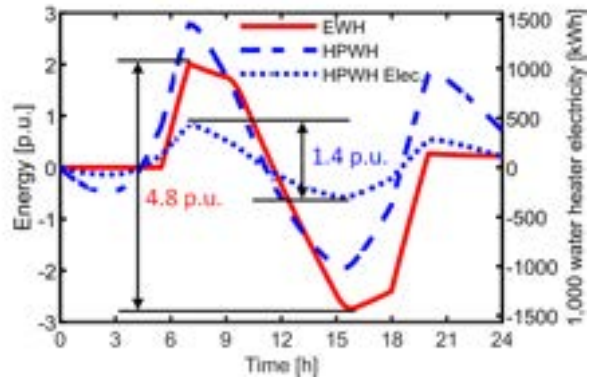

Fig. 24: The energy take for both EWHs and HPWHs with DR control. The energy take was high during the shedding periods because there was no energy input. In the afternoon, the energy take was negative, indicating the preheating process and higher water temperature in the tank. The corresponding electricity usage for HPWHs was lower due to the COP. The reserved capacities for both EWHs and HPWHs were approximately 22% of the corresponding daily electricity usage.

large reserved energy capacity for absorbing the surplus PV generation. The energy take went negative in the afternoon, indicating that the water was heated by the shifted load. The peak-to-peak values of the energy take in this example were 4.8 p.u. and 1.4 p.u., for EWH and HPWH, respectively. Given that the daily electricity usage for EWHs and HPWHs are 21.4 and 6.3, the reserved electric energy capacity for both EWHs and HPWHs were approximately 22% of their daily electricity usage. For a community with 1,000 EWHs, a total 2,500kWh energy can be stored in the water heaters in the example DR case. If the water heaters are all HPWHs, the number is approximately 730kWh.

VII. CONCLUSION

The proposed aggregated generic curves for residential water heaters, which use a minimal amount of data points, are the first of its kind to the best of the authors' knowledge. The aggregated generic curves for EWH and HPWH were

obtained based on large-scale projects. The experimental data for EWH generic curve was collected from approximately 800 users during a period of two years by the industrial collaborator, A.O. Smith. The experimental data for HPWH generic curve was provided by the BPA from the project involving 300 heat pump CTA-2045 enabled water heaters in the pacific northwest.

The experimental data was artificially aggregated in time and space and results show that the aggregated HPWH load had its daily power peak appear later than that of EWHs in both the morning and evening. The peak power for the aggregated EWH load was approximately 3 times that of the HPWH. The daily electricity usage of the aggregated EWH was approximately 3.4 times that of the HPWH.

The digital twin models for EWH and HPWH were created with the ability to calculate the water heating power, hot water flow, water temperature in the tank, and energy take for any number of water heaters. Case study results show that when referring to the average power, approximately 14% daily electricity usage for EWH could be shifted. Changing all EWH to HPWH reduces the daily electricity usage by approximately 70%. The HPWH still maintained the opportunity to shift approximately 17% of the daily electricity usage.

The potential of EWH and HPWH as energy storage was evaluated. The EWH could reserve the energy storage capacity equal to 22% of its daily electricity usage in the case study. Changing to HPWHs reduces the electric storage capacity because HPWHs use less electricity than EHWs in general. However, HPWHs still reserved capacity equal to 22% of their daily electricity usage when the peaks were shifted to the afternoon.

ACKNOWLEDGMENT

The support of A.O. Smith Corporation and of University of Kentucky, the L. Stanley Pigman endowment, is gratefully acknowledged.

References

[1] C. C. Hiller, "Comparing water heater vs. hot water distribution system energy losses," *ASHRAE transactions*, vol. 111, p. 407, 2005.

[2] H. Gong, V. Rallabandi, D. M. Ionel, D. Colliver, S. Duerr, and C. Ababei, "Dynamic modeling and optimal design for net zero energy houses including hybrid electric and thermal energy storage," *IEEE Transactions on Industry Applications*, 2020.

[3] Y. Liu, P. V. Etingov, S. Kundu, Z. Hou, Q. Huang, H. Zhou, M. Ghosal, D. P. James, J. Zhang, Y. Xie *et al.*, "Open-source high-fidelity aggregate composite load models of emerging load behaviors for large-sale analysis," Pacific Northwest National Lab.(PNNL), Richland, WA (United States), Tech. Rep., 2020.

[4] N. Carew, B. Larson, L. Piepmeier, and M. Logsdon, "Heat pump water heater electric load shifting: A modeling study," *Ecotope, Inc., Seattle*, 2018.

[5] "Residential Water Heater Training," http://university.hotwater.com/wp-content/uploads/sites/2/2015/02/un-branded-Residential-Training-Manual-1-5-16.pdf, accessed: 2020-10-27.

[6] N. Kruis, P. Bruce Wilcox, J. Lutz, and C. Barnaby, "Development of realistic water draw profiles for california residential water heating energy estimation," in *Proceedings of the 15th IBPSA Conference San Francisco, CA, USA, Aug. 7–9*, 2017.

[7] "CBECC-Res Compliance Software Project," http://www.bwilcox.com/BEES/cbecc2019.html, accessed: 2020-08-04.

[8] Q. Shi, C.-F. Chen, A. Mammoli, and F. Li, "Estimating the profile of incentive-based demand response (ibdr) by integrating technical models and social-behavioral factors," *IEEE Transactions on Smart Grid*, vol. 11, no. 1, pp. 171–183, 2019.

[9] B. Cui, J. Joe, J. Munk, J. Sun, and T. Kuruganti, "Load flexibility analysis of residential hvac and water heating and commercial refrigeration," Oak Ridge National Lab.(ORNL), Oak Ridge, TN (United States), Tech. Rep., 2019.

[10] H. Gong, O. M. Akeyo, T. Rooney, B. Branecky, and D. M. Ionel, "Aggregated generic load curve for residential electric water heaters," in *2021 IEEE Power & Energy Society General Meeting (PESGM)*. IEEE, 2021, pp. 1–5.

[11] H. Gong, V. Rallabandi, M. L. McIntyre, E. Hossain, and D. M. Ionel, "Peak reduction and long term load forecasting for large residential communities including smart homes with energy storage," *IEEE Access*, vol. 9, pp. 19 345–19 355, 2021.

[12] "CTA-2045 water heater demonstration report including a business case for cta-2045 market transformation," Bonneville Power Administration (BPA), Tech. Rep. BPA Technology Innovation Project 336, 2018.

[13] T. Clarke, T. Slay, C. Eustis, and R. B. Bass, "Aggregation of residential water heaters for peak shifting and frequency response services," *IEEE Open Access Journal of Power and Energy*, vol. 7, pp. 22–30, 2019.

[14] A. Doğan and M. Alçı, "Real-time demand response of thermostatic load with active control," *Electrical Engineering*, vol. 100, no. 4, pp. 2649–2658, 2018.

[15] M. A. Z. Alvarez, K. Agbossou, A. Cardenas, S. Kelouwani, and L. Boulon, "Demand response strategy applied to residential electric water heaters using dynamic programming and k-means clustering," *IEEE Transactions on Sustainable Energy*, vol. 11, no. 1, pp. 524–533, 2019.

[16] T. Peirelinck, C. Hermans, F. Spiessens, and G. Deconinck, "Domain randomization for demand response of an electric water heater," *IEEE Transactions on Smart Grid*, vol. 12, no. 2, pp. 1370–1379, 2020.

[17] O. E. Bosaletsi and W. Cronje, "Decentralized control scheme applied to domestic electric water heaters to minimize frequency deviations: Initial results." in *2021 Southern African Universities Power Engineering Conference/Robotics and Mechatronics/Pattern Recognition Association of South Africa (SAUPEC/RobMech/PRASA)*. IEEE, 2021, pp. 1–6.

[18] J. Wang, H. Zhang, Y. Zhou, J. Sun, and D. Wang, "Evaluation of the potential regulation capacity of water heater loads," in *2013 5th International Conference on Power Electronics Systems and Applications (PESA)*. IEEE, 2013, pp. 1–5.

[19] G. C. Heffner, C. A. Goldman, and M. M. Moezzi, "Innovative approaches to verifying demand response of water heater load control," *IEEE Transactions on Power Delivery*, vol. 21, no. 1, pp. 388–397, 2005.

[20] J. Kondoh, N. Lu, and D. J. Hammerstrom, "An evaluation of the water heater load potential for providing regulation service," in *2011 IEEE Power and Energy Society General Meeting*. IEEE, 2011, pp. 1–8.

[21] V. Lakshmanan, H. Sæle, and M. Z. Degefa, "Electric water heater flexibility potential and activation impact in system operator perspective–norwegian scenario case study," *Energy*, p. 121490, 2021.

[22] X. Xu, C.-f. Chen, X. Zhu, and Q. Hu, "Promoting acceptance of direct load control programs in the United States: Financial incentive versus control option," *Energy*, vol. 147, pp. 1278–1287, 2018.

[23] "American Council for an Energy-Efficient Economy (ACEEE): Hot Water Forum," https://www.aceee.org/2021-hot-water-forum, accessed: 2021-08-12.

[24] "CTA standard: Modular communications interface for energy management," Consumer Technology Association (CTA), Tech. Rep., 2020.

[25] X. C. Katherine Dayem, "Standardized Communications for Demand Response: An Overview of the CTA-2045 Standard and Early Field Demonstrations," National Rural Electric Cooperative Association (NRECA), Tech. Rep., 2018.

[26] "Energy Star water heaters - test method to validate demand response," https://www.energystar.gov/products/spec/residential_water_heaters_specification_version_3_0_pd, accessed: 2021-08-12.

[27] C.Thomas, "Performance test results: CTA-2045 water heater," Electric Power Research Institute (EPRI), Tech. Rep. 3002011760, 2017.

[28] "Energy Smart Electric Water Heater Controller: Installation, Operation and Troubleshoooting Instructions," https://www.lowes.com/pdf/Energy_Smart_Electric_Water_Heater_Controller.pdf, accessed: 2021-08-12.

[29] "Reginal study of cta-2045 enabled water heaters," https://www.bpa.gov/EE/Technology/demand-response/Pages/CTA2045-DataShare.aspx, accessed: 2021-06-24.
[30] "Energy Plus Documentation: Engineering Reference," https://energyplus.net/assets/nrel_custom/pdfs/pdfs_v9.5.0/EngineeringReference.pdf, accessed: 2021-09-08.
[31] V. R. Salcido, Y. Chen, Y. Xie, and Z. T. Taylor, "Energy Savings Analysis: 2021 IECC for Residential Buildings," Pacific Northwest National Laboratory (PNNL), Tech. Rep., 2021.
[32] "Ecotope Research: HPWHsim," https://github.com/EcotopeResearch/HPWHsim, accessed: 2021-09-08.
[33] H. Gong, E. S. Jones, A. H. M. Jakaria, A. Huque, A. Renjit, and D. M. Ionel, "Generalized energy storage model-in-the-loop suitable for energy star and cta-2045 control types," in *2021 IEEE Energy Conversion Congress and Exposition (ECCE)*. IEEE, 2021, pp. 1–5.
[34] "American Council for an Energy-Efficient Economy (ACEEE): Hot Water Forum Program," https://www.aceee.org/sites/default/files/pdfs/hwf21-final_program-3.8.pdf, accessed: 2021-08-12.

HUANGJIE GONG (S'18) received the B.Eng. degree in automation from Harbin Engineering University, Harbin, China, in 2013 and the M.S. degree in control theory and control engineering from Southwest Jiaotong University, Chengdu, China, in 2016. Since 2017 he is a Ph.D. student in the SPARK Laboratory, ECE Department at University of Kentucky, Lexington, KY, USA, where he has been working on research projects sponsored by DOE, NSF, Electric Power Research Institute (EPRI), industry and utilities. He is the main developer of a large-scale co-simulation software framework for energy in buildings and power flow in electric distribution systems. In 2021, he was a graduate student intern with the National Renewable Energy Laboratory (NREL). He is an executive committee member for the joint student chapter at UK and a member of PES renewable energy generation subcommittee. His research interests include renewable energy integration, modeling and control of energy storage, batteries, water heaters, HVAC systems, EV, net zero energy (NZE) buildings, and microgrids.

TIM ROONEY received a B.S. in Mechanical Engineering in 2017 and an M.S. in Engineering in 2019, both from the University of Wisconsin - Milwaukee. He is currently employed as a Senior Project Engineer at the A. O. Smith Corporate Technology Center in Milwaukee, WI, where he is focused on the areas of data acquisition, data analysis, and optimization through water heater performance modeling and simulation.

OLUWASEUN M AKEYO (S'16 – M'21) received the Ph.D and M.S. degree in electrical engineering from the University of Kentucky, Lexington, KY, USA in 2017 and 2020, respectively, and the B. Eng degree in electrical and electronics engineering from Abubakar Tafawa Balewa University (ATBU), Bauchi, Nigeria in 2014. He is currently a Senior Associate Engineer with Sargent & Lundy, where he focuses on renewable system integration, and transmission and distribution system analysis. He has published more than fifteen peer-reviewed journal papers and conference proceedings, which include one that received a Best Poster/Paper Award at the 2016 IEEE International Conference on Renewable Energy Research and Applications (ICRERA) in Birmingham, England, and one that received the 2020 IEEE Industry Applications Society RES Committee Transactions Paper Award - Third Prize for integration studies of large battery energy storage systems into multi-MW grid connected PV systems.

BRIAN T. BRANECKY received the B.S. and M.S. degrees in electrical engineering from Texas Tech University in 1986 and University of Wisconsin–Milwaukee in 1998. He is presently employed as an Engineering Fellow at the A. O. Smith Corporate Technology Center where his main areas of interest include thermal energy management, system modeling and internet connected appliances. Brian has several patents related to water heater controls enrolled in utility demand response programs.

DAN M. IONEL (M'91–SM'01–F'13) received the M.Eng. and Ph.D. degrees in electrical engineering from the Polytechnic University of Bucharest, Bucharest, Romania. His doctoral program included a Leverhulme Visiting Fellowship with the University of Bath, Bath, U.K and he later was a Postdoctoral Researcher with the SPEED Laboratory, University of Glasgow, Glasgow, U.K.

Dr. Ionel is a professor of electrical engineering and the L. Stanley Pigman Chair in Power with the University of Kentucky, Lexington, KY, USA, where he is also the Director of the Power and Energy Institute of Kentucky and of the SPARK Laboratory. He previously worked in industry for more than 20 years. Dr. Ionel's current research group projects on smart grid and buildings, and integration of distributed renewable energy resources and energy storage in the electric power systems are sponsored by NSF, DOE, industry and utilities. He published more than 200 technical papers, including some that received IEEE awards, was granted more than 30 patents, and is co-author and co-editor of the book "Renewable Energy Devices and Systems – Simulations with MATLAB and ANSYS", CRC Press.

Dr. Ionel received the IEEE PES Veinott Award, was the Inaugural Chair of the IEEE IAS Renewable and Sustainable Energy Conversion Systems Committee, an Editor for the IEEE TRANSACTIONS ON SUSTAINABLE ENERGY, and the Technical Program Chair for IEEE ECCE 2016. He is the Editor in-Chief for the Electric Power Components and Systems Journal, and the Chair of the Steering Committee for IEEE IEMDC.